Atmospheric Environment 115 (2015) 9–18

Contents lists available at ScienceDirect

Atmospheric Environment

journal homepage: www.elsevier.com/locate/atmosenv

Understanding interannual variations of biomass burning from Peninsular Southeast Asia, part II: Variability and different influences in lower and higher atmosphere levels

Xinyi Dong, Joshua S. Fu*

Department of Civil and Environmental Engineering, The University of Tennessee, Knoxville, TN, 37996, USA

HIGHLIGHTS

- Upper and lower limit of PSEA biomass burning impact and its interannual variation are examined.
- Uplift of biomass burning is examined and lee side trough play major role instead of deep convection.
- Biomass burning may have little impact in PBL but contribute 30% to free troposphere O_3 at Taiwan.

ARTICLE INFO

Article history:
Received 5 January 2015
Received in revised form
21 May 2015
Accepted 24 May 2015
Available online 27 May 2015

Keywords:
Peninsular Southeast Asia
Biomass burning
Interannual variation
Uplift transport

ABSTRACT

A synthetic study including model, ground observation, sounding profiles, and satellite retrievals was applied to investigate the interannual variations of biomass burning from Peninsular Southeast Asia (PSEA) in terms of its emission, transport and impacts over the local and downwind areas. Study period ranged from 2006 to 2010 during March and April which was the PSEA biomass burning season. Analysis of geopotential height indicated that PSEA biomass burning plume was rapidly uplifted by the lee side trough over Yungui Plateau into free troposphere which favors the long-range transport down to East Asia (EA). Lightning data from NASA demonstrated deep convection was weak over PSEA during the burning season and it may only play a minor role for uplifting. Although PSEA biomass burning had large annual variation such as the emission in 2010 was 65% higher than that in 2008, its impact at near surface layer for CO, O_3 and $PM_{2.5}$ within 0–1 km height had less variability since most of the plume was uplifted into free troposphere. At lower part of free troposphere within 1 km–3 km however, impact of PSEA biomass burning at downwind areas showed consistent annual variations with the emission changes. Sounding observations demonstrated PSEA biomass burning may have almost no impact on the near surface layer O_3 over Taiwan but contributed more than 30% of O_3 at free troposphere within 1–6 km height during massive burning events. PSEA biomass burning also significantly affected aerosol optical depth (AOD) over EA, with the contributions ranged from 0.1 to 0.3 (25%–45% in total AOD) in 2008 to 0.2–0.6 (50%–70% in total AOD) in 2010. Our analysis indicated that although PSEA biomass burning may have relatively stable impact on air quality over EA from year to year, it will cause significant disturbance to the free troposphere over EA for both atmospheric chemistry and radiative forcing budget.

1. Introduction

Biomass burning is one of the most important sources for many different types of aerosols including organic carbon, black carbon, soot, and secondary inorganic aerosols in PSEA (Lin et al., 2013; Reid et al., 2013). As indicated by 2007 IPCC report (IPCC, 2007), these aerosols may have significant impact on the regional climate, biodiversity, coastal ecosystem, and land degradation, yet the understanding of biomass burning over Southeast Asia (SEA) contain large uncertainties due to the complexities of geography, meteorology, and hydrology, and also lack of research efforts in this area. SEA contains two major continents, the Maritime Continent (MC: Indonesia, Philippines, and Papua New Guinea) and Peninsular Southeast Asia (PSEA: Cambodia, Laos, Myanmar, Thailand,

* Corresponding author.
E-mail address: jsfu@utk.edu (J.S. Fu).

http://dx.doi.org/10.1016/j.atmosenv.2015.05.052
1352-2310/

Vietnam; PSEA is also referred as Indochina in some literatures), and both of them have intensive biomass burning largely due to agricultural activities. Although a few studies have investigated biomass burning in MC due to its dominant impact on visibility reduction (Reid et al., 2012; van der Werf et al., 2008; van der Werf et al., 2004), biomass burning in PSEA remain poorly understood due to its environmental and political complexity. Although MC and PSEA share many similarities such as complex topography and high cloud coverage, they also differ significantly with different regional climates. MC is under control of Intertropical Convergence Zone (ITCZ) with a typical almost year around hot and wet condition and often affected by volcanoes as another important aerosol source (Halmer et al., 2002; Nho et al., 1996; Symonds et al., 1987), and PSEA is controlled by both ITZC and monsoon systems thus have clearly distinguished dry and wet seasons. Due to different climates, biomass burning season covers July to October at MC and February to April at PSEA. In recent years, some international field experiments have been conducted aiming at help understand the characteristics and impacts of biomass burning on both climate and air quality over PSEA. The NASA TRACE-P (Jacob et al., 2003) campaign conducted in 2001 tried to quantify the biomass burning emission and impacts on air quality; the UNEP ABC/EAREX2005 campaign (Nakajima et al., 2007) conducted in 2005 investigated the aerosols impact on aerosol optical thickness (AOT) and single scattering albedo (SSA); NASA and Taiwan collaborated the BASE-ASIA and 7-SEAS/Dongsha experiment campaigns (Li et al., 2013; Tsai et al., 2013) and performed interdisciplinary studies examining the chemical, physical, and radiative properties of biomass burning aerosols over PSEA.

Although these research efforts allow us to probe into some fundamental characteristics of biomass burning over PSEA, many of them focus on massive events and lack of systematic evaluation of the interannual variations, which may have substantial changes due to different driving forces from both meteorological and human activities. For example, extreme episodes such as the El Nino event in 2006 can lead to more than 30 times of biomass burning carbon emission than La Nina event in 2000 at Borneo (van der Werf et al., 2008). Throughout PSEA most of the biomass burning fires are originated by anthropogenic activities for land use purposes. While this area has seen rapid economic growth, various factors such as economical, social, and even political, may lead to changes of fire activities. Reid et al. (2013) suggested that as many of PSEA countries' economic rely on oil palm plantation farming and fire is usually employed as a popular toll as regeneration for every 10–20 years, a pulse of agricultural burning might be expected accordingly.

While field measurements or campaigns are limited by temporal and spatial coverage, and satellite retrievals still contain a large fraction of uncertainties especially over PSEA due to the high cloud cover, modeling can serve as a complementary tool to help explore biomass burning in this area. Despite some published studies (Deng et al., 2008; Fu et al., 2012; Huang et al., 2013; Tang et al., 2003) focusing on massive events, modeling efforts are still limited to understand the characteristics of PSEA biomass burning, such as its upper and lower limits and annual variability. The purpose of this study is to continuously in the Part I investigate the interannual changes of biomass burning over PSEA in terms of emission, transport, and impact at local and downwind area with the 3-D modeling system WRF/CMAQ. In particular, we examined the impact of biomass burning at different atmosphere levels, which provide fundamental information for understand the chain-effect on atmospheric chemistry and also help probe into the impact on radiative forcing budget over East Asia (EA). The WRF/CMAQ modeling system was applied for 5 consecutive years from 2006 to 2010 during the biomass burning season (March and April). Section 2 briefly introduced the simulation design and annual changes of biomass burning emission over PSEA; section 3 discussed the uplift scheme and transport pathway of biomass burning, the upper and lower limit of the impacts, and the different contributions at near surface layer and lower part of free troposphere; and Section 42 summarized the findings as well as indications from this study.

2. Simulation scenarios and emissions

2.1. Simulation scenarios

Community Multiscale Air Quality (CMAQv5.0.1) modeling system developed by US EPA (Byun and Schere, 2006) and scientific community and the Weather Research Forecasting (WRFv3.3) model (Skamarock et al., 2008) were selected as modeling platform, and detailed introduction about emission inventories and model evaluation are summarized in Dong and Fu (2015). In order to evaluate the impact of biomass burning, base case scenario with all the emissions (BASE) and sensitivity scenario without biomass burning emission (NOBIO) are defined. The difference between these two scenarios (NOBIO − BASE) thus describes the contribution from biomass burning. Simulation period for different scenarios are same, covering March and April from 2006 to 2010.

2.2. Annual variations of biomass burning emission

PSEA is a very vulnerable area to regional climate change, and oscillations of meteorology may have large impacts on fire activity. Since biomass burning emission over PSEA may also vary from year to year, it's necessary to examine the emission intensities during the study period. Fig. 1 summarized the monthly carbon emission in March and April from biomass burning derived from FLAMBE inventory (Reid et al., 2009) utilized in this study. We focused on these two months only because over PSEA, they comprise the dry season with high temperature and few precipitation, and PSEA fire activities usually start in late December and peak in March and April, followed by a sharp decrease with monsoon onset in May.

Fig. 1 indicated notable interannual variation of biomass burning emission especially in March, while April had much less variability. Emission in March 2010 and 2008 was 489 Tg and 191 Tg respectively, suggesting significant annual changes by a factor of 2 for monthly emission. Total emission in 2010 was about 65% higher than that in 2008. Fire was widely applied for various purposes in PSEA, including deforestation, open fire burning of agricultural waste/residual, and swidden cultivation, and these activities are more or less affected by precipitation. Although there have been

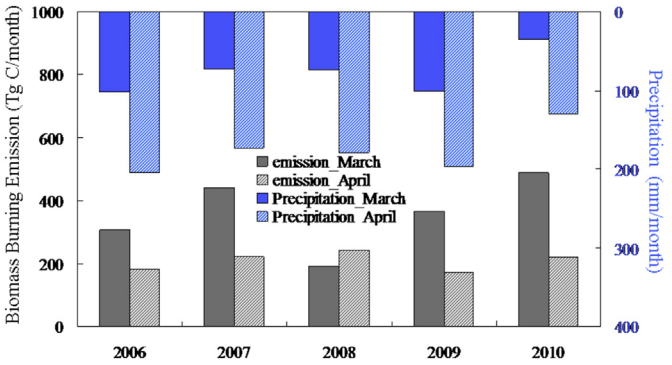

Fig. 1. Monthly averages of biomass burning emission (gray bars) and precipitation (blue bars) in March (solid bars) and April (dash bars) from 2006 to 2010. (For interpretation of the references to color in this figure legend, the reader is referred to the web version of this article.)

extensive published work focusing on MC which explained the relationships between ENSO, negative precipitation anomalies, and overall fire activity (Nichol, 1998), such kind of work has not been performed for PSEA to systematically examine the annual variability of biomass burning and the driving forces behind. Over MC, interannual variability of fire-driven deforestation rates were found partly due to changes of precipitation (van der Werf et al., 2008), but for PSEA the relationship between burning behavior and the meteorology remain largely un-documented. Cook and Buckley (2009) reported that monsoonal behavior in Thailand was only weakly coupled with ENSO. Tsai et al. (2013) reported anti-correlation between precipitation and biomass burning for overall SEA based on GFED inventory, but many exceptions such as increasing precipitation and emission from 2008 to 2009 also suggested the cause-and-effect relationship remain unknown. As indicated by the monthly average precipitation shown in Fig. 1, correlation between biomass burning emission and precipitation was −0.77 during the 5 simulation years. Precipitation declined significantly from 2006 to 2007 and from 2009 to 2010, where the emissions were also found to increase in 2007 and 2010, suggesting that precipitation was negatively correlated with biomass burning emission. However, we also found that highest precipitation may not necessarily indicate lowest biomass burning emission. For example, the highest monthly average precipitation in March was 101 mm in 2006, but lowest emission was in 2008. March 2008 had only 73 mm precipitation yet the lowest emission among the 5 years. In addition, both precipitation and emission was increased from 2008 to 2009 in March, which was also consistent with the exceptions reported by Tsai et al. (2013), suggesting that the precipitation variability can not fully explain the interannual changes of biomass burning over PSEA. To our knowledge there is no examination of the extreme biomass burning at PSEA in 2008 and 2010 in peer-reviewed publications. In fact, despite a few different research efforts that have identified the variability of biomass burning from year to year on global scale, the exact causes for emission's variability also remain unclear for other biomass burning areas as well (van der Werf et al., 2010). Torres et al. (2010) reported that in South America, 2008 precipitation is very similar to that in 2005 which had the most intense biomass burning in the past 10 years, yet 2008 had surprisingly weak emission. A similar pattern was found for PSEA as both 2007 and 2008 there was relatively lower precipitation in March, yet biomass burning emission was substantially higher in 2007 but not in 2008. Thus explicit understanding of the driving force of biomass burning emission change remain an open-ended question.

3. Results and discussions

3.1. Uplift and transport of PSEA biomass burning

As introduced in Section 2, the difference between BASE case and the sensitivity case NOBIO represented the contribution from biomass burning. Fig. 2(a) and (b) summarized the spatial distribution of biomass burning O_3 (from BASE-NOBIO) at near surface layer (0–1 km) and high layer (1 km–3 km) respectively, with white dashed contour lines denote the percentage contribution due to biomass burning in March 2006. These two levels are selected because the planetary boundary layer (PBL) was around 1 km height over PSEA and EA, and 1–3 km is investigated to represent the lower part of free troposphere. We used the data of this month to illustrate the spatial coverage and transport of PSEA biomass burning as other months are similar and only differ in terms of intensity. As indicated by Fig. 1(a), biomass burning in PSEA can spread from the local source region (90°E–105°E) down to Southern China (105°E–120°E) and West Pacific (>120°E). In local area, biomass burning contributed more than 60% (~50 ppbv) of total surface O_3 in Myanmar, Laos, and northern Thailand, the impact declined gradually from 20% (~15 ppbv) at Vietnam to about 5%–10% (~5 ppbv) over south China and Taiwan. Although many of the intensive emission sources are located between 20°N and 25°N latitude, influence of biomass burning was confined below 30°N latitude and could not transport too far towards north within boundary layer. Huang et al. (2013) demonstrated the westerlies wind pattern dominated the eastward transport of biomass burning, but impacts of PSEA biomass burning spread further on the south side down to 5°N. Also, there was a drastic decrease of biomass burning influence from 40% to 20% over Yungui Plateau from 100°E to 105°E longitude as shown in Fig. 1(a). At 1–3 km height as shown in Fig. 1(b), impact of biomass burning can transport eastward further at downwind areas. Contribution by biomass burning can reach up to 25% (30 ppbv) in South China within 1–3 km height, although it could not transport northward further than 30°N latitude either. To examine the upward transport of biomass burning plumes, Fig. 2(c) and (d) summarized the O_3 flux at 0–1 km and 1–3 km respectively. Here O_3 flux was defined as the multiply product of biomass burning O_3 concentration with unit of $\mu g/m^3$ and wind speed with unit of m/s, so the unit for O_3 flux is $\mu g/m^2 s$, which described the O_3 outflow from PSEA at different atmosphere levels. As shown in Fig. 2(c), two major surface level streams, one from the south leeside flank of Tibet Plateau and another from west Pacific meet together at the south edge of Yungui Plateau and preserve most of the biomass burning O_3 within this area. The combined surface stream then stated to move northward and trapped in Sichuan Basin area following the topography as shown in Fig. 2(e). Higher terrain height at north side of Sichuan Basin blocked northward transport of biomass burning and kept the surface level O_3 from PSEA biomass burning remain lower than 30°N latitude. Transport of O_3 flux in layers 1–3 km height was different as shown in Fig. 2(d). The westerly from south flank of Tibet Plateau dominated the eastward transport of elevated O_3, which had no topography blocks or resistance from pressure system. In fact, the West Pacific High Pressure system favored eastward transport at 1–3 km height as shown in Fig. 2(d), and the intensity of O_3 flux in free troposphere was also larger than that in lower atmosphere, indicating that PSEA biomass burning had a more significant impact in higher atmospheric level than in the near-surface layer over downwind areas.

Understanding of the PSEA biomass burning upward transport mechanism was not well developed due to limited research efforts. Liu et al. (2003) claimed that deep convection is the dominate factor for PSEA biomass burning outflow based on GEOS-Chem simulation, and a few studies mentioned the deep convection as the driving force but without verifying this issue. Lin et al. (2009) used tracer module in WRF/Chem and showed that when leeside trough was formed at eastern flank of Tibet Plateau over PSEA, it can uplift biomass burning plumes to 3 km height above ground. However, the simulations conducted by Lin et al. (2009) artificially assigned O_3 to fire locations identified by MODIS in the first model layer only (~20 m), and O_3 was treated as a non-reactive tracer. While the real biomass burning emission was demonstrated to have different injection heights depending on burning activities and time-dependent temporal profile (Jian and Fu, 2014), simulations by Lin et al. (2009) may contain large uncertainties. In this study the real 3-D WRF/CMAQ simulation with FLAMBE emission inventory which contained hourly profile and estimated injection height based on SMOKE (Huang et al., 2013) provided a more solid dataset to examine the uplift and transport of biomass burning O_3 at PSEA. Fig. 2(f) showed the cross sectional contour of biomass burning O_3 concentration (filled color contours) and percentage contribution (dash white lines with red labels), wind vectors (black

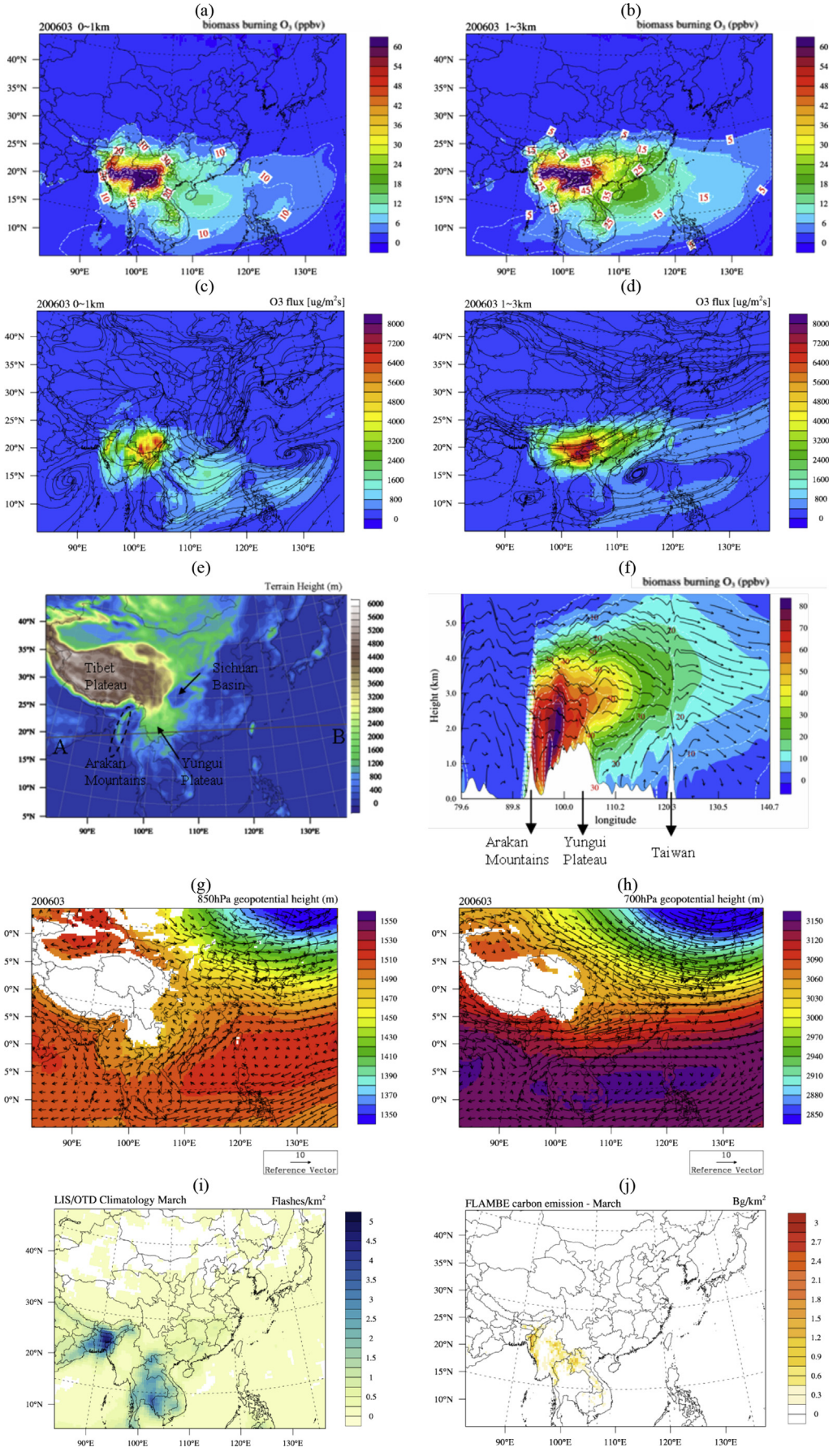
(a)
200603 0~1km
biomass burning O3 (ppbv)
(b)
200603 1~3km
biomass burning O3 (ppbv)
(c)
200603 0~1km
O3 flux [ug/m2s]
(d)
200603 1~3km
O3 flux [ug/m2s]
(e)
Terrain Height (m)
Tibet Plateau
Sichuan Basin
Arakan Mountains
Yungui Plateau
A
B
(f)
biomass burning O3 (ppbv)
Height (km)
longitude
Arakan Mountains
Yungui Plateau
Taiwan
(g)
200603
850hPa geopotential height (m)
Reference Vector
(h)
200603
700hPa geopotential height (m)
Reference Vector
(i)
LIS/OTD Climatology March
Flashes/km2
(j)
FLAMBE carbon emission - March
Bg/km2

curly vectors, with vertical wind speed scaled based on the ratio between average horizontal and vertical winds), and terrain height following the brown line AB shown in Fig. 2(e). Biomass burning emissions were mainly located between 90 and 105°E longitude (Myanmar, north Thailand, Laos, and Vietnam), where the uplift motion helped to bring excessive O_3 up to 6 km in the free troposphere, and then the westerly helped to transport it eastward down to West Pacific around 140°E longitude. Fig. 2(g) and (h) showed the geopotential height (GPH, represented as filled color contours) overlaid with wind vectors (black curly vectors) at 850 hPa and 700 hPa respectively, and both of them demonstrated the existence of the trough along the eastern lee side of Tibet Plateau over Yunnan and Guizhou provinces of China (Yungui Plateau). At PSEA where the trough was laid between Bay of Bengal and South China Sea, wind directions were changed from northwest to southeast along the edge of the trough at Myanmar, northern Thailand, and Laos at 850 hPa, which was right over the source area of biomass burning. The existence of lee side trough indicated its importance for uplifting biomass burning. With the elevated terrain biomass burning plume was driven by the trough and uplifted into free troposphere over Yungui Plateau. On the other hand, the NASA Lightning Image Sensor and Optical Transient Detector (LIS/OTD) data suggested lightning over PSEA was weak in March as shown in Fig. 2(i). Lightning was used here as an indicator for the existence of deep convection to distinguish it from the large scale convection caused by trough. Locations and intensity of biomass burning were shown in Fig. 2(j). Weak lightning occurred at west side of Arakan Mountains due to the impact of southwestern monsoon, yet biomass burning was located at east side as demonstrated in Fig. 2(f) and (j). Over south edge of Yungui Plateau, weak lightning was also found at north Laos and Vietnam which was the biomass burning source area. Fig. 2(f) suggested that strong uplift motion occurred within 95°E–100°E longitude, which was at eastern Myanmar and had almost no lightning in March. The existence of large scale lee side trough and the weak intensity of lightning indicated that trough should be the dominate contributor for uplifting biomass burning in PSEA, and deep convection only played minor role over north Laos and Vietnam. Transport of biomass burning in April was similar to March except that more lightning was found over northern Laos and Vietnam indicating stronger deep convections over Yungui Plateau.

3.2. Annual variations of PSEA biomass burning impacts

As Section 2 demonstrated the substantial interannual variability of biomass burning emission, its impact may also change accordingly. Among the 5 simulation years in this study, emission was lowest in 2008 and highest in 2010, so we compared the 5-years average with the minimum and maximum impacts from 2008 to 2010 respectively to examine the average, upper and lower limit of biomass burning impacts in local and downwind areas, as shown in Fig. 3.

Fig. 3 summarized the absolute concentration changes (filled color contour) and percentage contributions (white dash lines with red labels) from biomass burning at the near surface layer (0–1 km) for O_3 (1st row), $PM_{2.5}$ (2nd row), and CO (3rd row) respectively, with the comparison between 5-years average (left column), the minimum (2008, middle column) and maximum (2010 right column) values. For the 5-years average impacts as shown in Fig. 3(a), biomass burning contributed 20 ppbv–60 ppbv (10%–50%, values in the parentheses wither percentage sigh refers to the percentage contribution here and after) of total O_3 at source region, 8 ppbv–26 ppbv (12%–24%) at South China, and 5 ppbv–10 ppbv (4%–12%) at West Pacific. The comparison with minimum and maximum values shown by Fig. 3(b) and (c) respectively suggested that although the contributions over source area changed from less than 45 ppbv in 2008 to more than 60 ppbv in 2010, the impacts over downwind areas had no sizable changes. PSEA biomass burning had similar impacts for O_3 in 2008 and 2010 as 3 ppbv–10 ppbv (4%–12%) over Taiwan. The contributions for $PM_{2.5}$ and CO had similar spatial distributions and annual changes shown in Fig. 3(d)–(i). For 5-years average impacts, PSEA biomass burning contributed 15 μg/m^3–35 μg/m^3 (25%–50%), 5 μg/m^3–8 μg/m^3 (16%–20%), and 0–5 μg/m^3 (0–16%) for $PM_{2.5}$ at source region, south China, and West Pacific respectively, and the contributions for CO were 400 ppbv–600 ppbv (35%–60%), 200 ppbv–300 ppbv (20%–35%), and 50 ppbv–150 ppbv (5%–30%) respectively. The impacts at source region ranged from 25 μg/m^3 and 350 ppbv in 2008 to more than 40 μg/m^3 and 600 pbv in 2010 for $PM_{2.5}$ and CO respectively, while the impacts at South China and West Pacific were found have no significant differences between 2008 and 2010 as compared to 5-years averages. Considering the biomass burning emission at PSEA in 2010 was 65% higher than that in 2008, its impact at near surface layer at downwind area had no significant annual variations.

To verify the variability of biomass burning contribution at downwind area, we also investigated surface observations of CO, O_3, and $PM_{2.5}$ at Hong Kong and Taiwan, both of which were located along the transport pathway. Fig. 4 demonstrated the daily averages of observations (color cycles) against simulated total concentrations (black lines: sim_total) and the contributions from biomass burning (blue lines: sim_BB). As suggested by Fig. 4, observations generally agreed well with modeled total concentrations of pollutants at both Hong Kong and Taiwan, and the contributions of biomass burning had no drastic annual variation. At Hong Kong, contributions from biomass burning for CO, O_3, and $PM_{2.5}$ ranged from 117 ppbv(19.5%), 7.2 ppbv(13.8%), and 4.3 μg/m^3 (11.7%) respectively in 2008 to 164 ppbv(27.1%), 9.1 ppbv(18.3%), and 5.1 μg/m^3 (17.2%) respectively in 2010. As compared to emissions which had significant interannual variability by 65%, contribution of PSEA biomass burning had less annual changes by 30%–40% over Hong Kong. The interannual variation of biomass burning impact at Taiwan was found even smaller, with contribution for CO, O_3, and $PM_{2.5}$ ranged from 61 ppbv (10.5%), 3.2 ppbv (11.3%), and 3.7 μg/m^3 (9.7%) respectively in 2008 to 90 ppbv (15.1%), 4.1 ppbv (16.1%), and 5.9 μg/m^3 (14.1%) respectively in 2010. The uplift motion discussed in Section 3.1 demonstrated that major part of biomass burning was uplifted and remain in free troposphere, which explained the weak interannual variability of its impact at near surface layer at downwind areas including South China and West Pacific.

We also examined the impacts within lower part of free troposphere at 1 km–3 km height and found the contributions differ significantly at South China and West Pacific for different years, as shown in Fig. 5. Fig. 5 was similar to Fig. 3, but summarized the changes at higher levels. For 5-years average, PSEA biomass burning contributed to 30 ppbv–55 pbv (25%–50%),

Fig. 2. Monthly averages (March 2006) for: biomass burning O_3 concentration (color contour) and percentage contributions (white dash lines with red labels) at (a). 0–1 km and (b). 1–3 km height; O_3 flux at (c). 0–1 km and (d). 1–3 km height, with color contours represented the flux intensity and curly vectors represented the flux direction; (d). terrain height; (f). vertical cross section (following the brown line AB shown in Fig. 2(d)) of biomass burning O_3 concentration (color contours) and percentage contribution (white dash lines with red labels), wind vector (curly vectors, with vertical wind scaled based on the ratio between vertical and horizontal wind speed) and terrain height; and geopotential height at (g). 850 hPa and (h). 700 hPa; (i) LIS/OTD climatology lightning intensity; (j). FLAMBE carbon emission. (For interpretation of the references to color in this figure legend, the reader is referred to the web version of this article.)

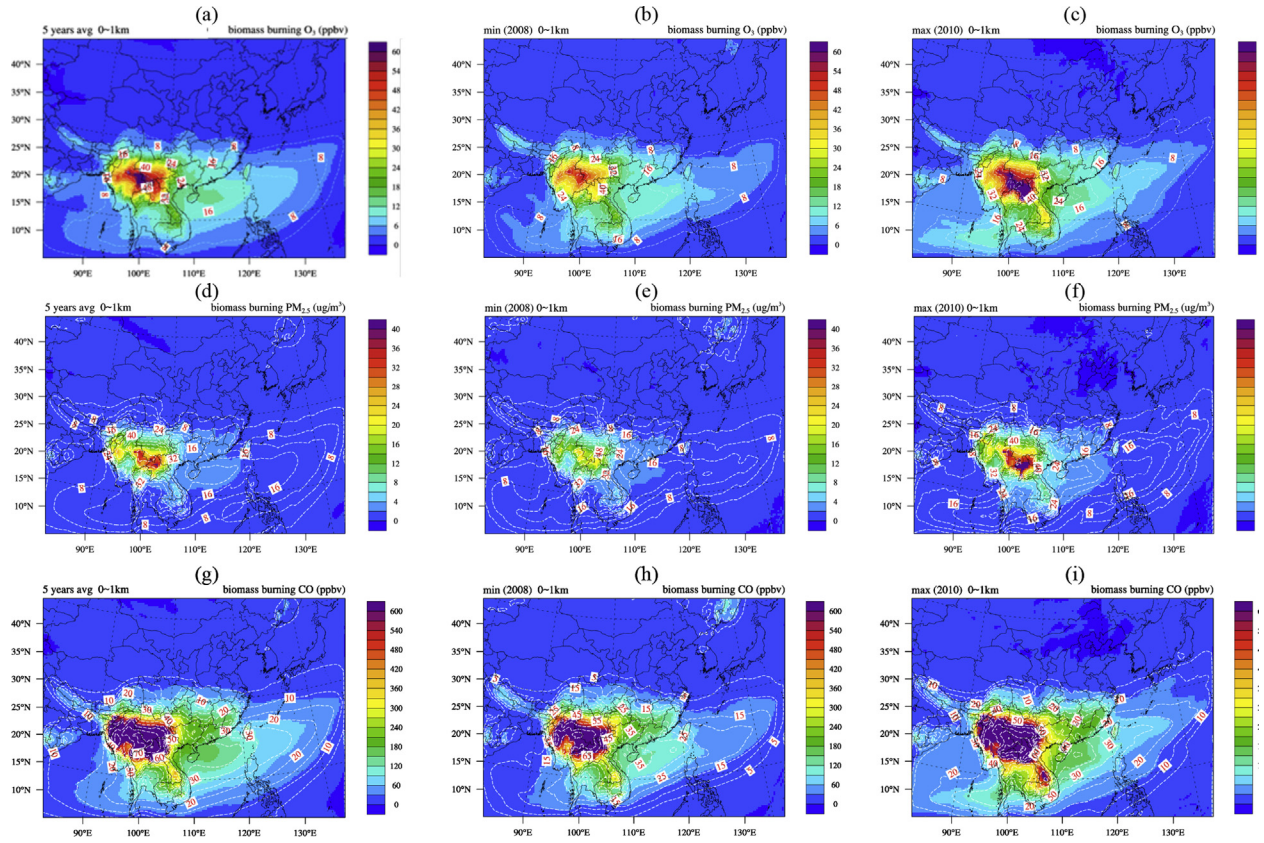

Fig. 3. Biomass burning impacts at near surface layer (0–1 km) for O_3 (1st row), $PM_{2.5}$ (2nd row), and CO (3rd row) for 5-years average during biomass burning season in March and April (1st column), 2008 with lowest biomass burning emission representing the minimum impacts (middle column), and 2010 with highest biomass burning emission representing the maximum impacts (right column). Concentrations are plotted with filled color contours and percentage contributions are denoted by white dash lines with red labels. (For interpretation of the references to color in this figure legend, the reader is referred to the web version of this article.)

15 ppbv–40 pbv (20%–40%), and 0–15 ppbv (0–20%) for O_3 at source region, South China, and West Pacific respectively. In 2008 contribution for O_3 was 25 ppbv–45 ppbv (20%–40%), 10 ppbv–30 ppbv (15%–30%), 0–10 ppbv (0–15%) over source area, South China, and West Pacific respectively, and in 2010 the values are 35 ppbv–60 ppbv (30%–55%), 25 ppbv–45 ppbv (20%–45%), 0–20 ppbv (0–20%) respectively. Unlike the near-surface level which didn't show sizable changes from 2008 to 2010, the higher

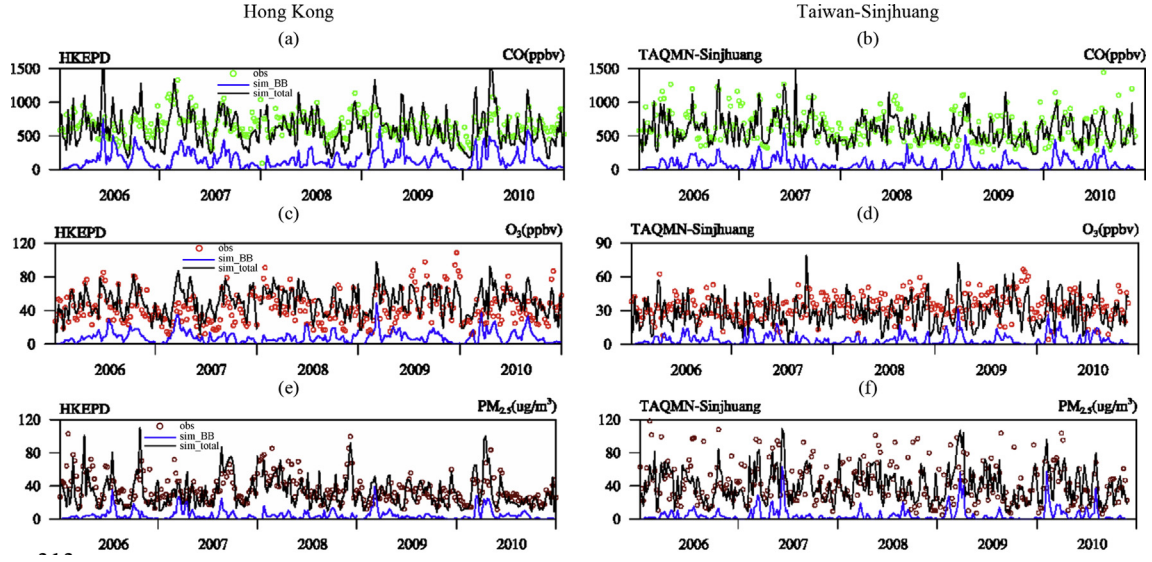

Fig. 4. Daily averages of CO (1st row), O3 (2nd row), PM2.5 (3rd row) at Hong Kong (left column) and Taiwan-Sinjhuang (right column) from observation (color cycles), modeled total concentrations (black lines: sim_total), and contributions from biomass burning (blue lines: sim_BB). (For interpretation of the references to color in this figure legend, the reader is referred to the web version of this article.)

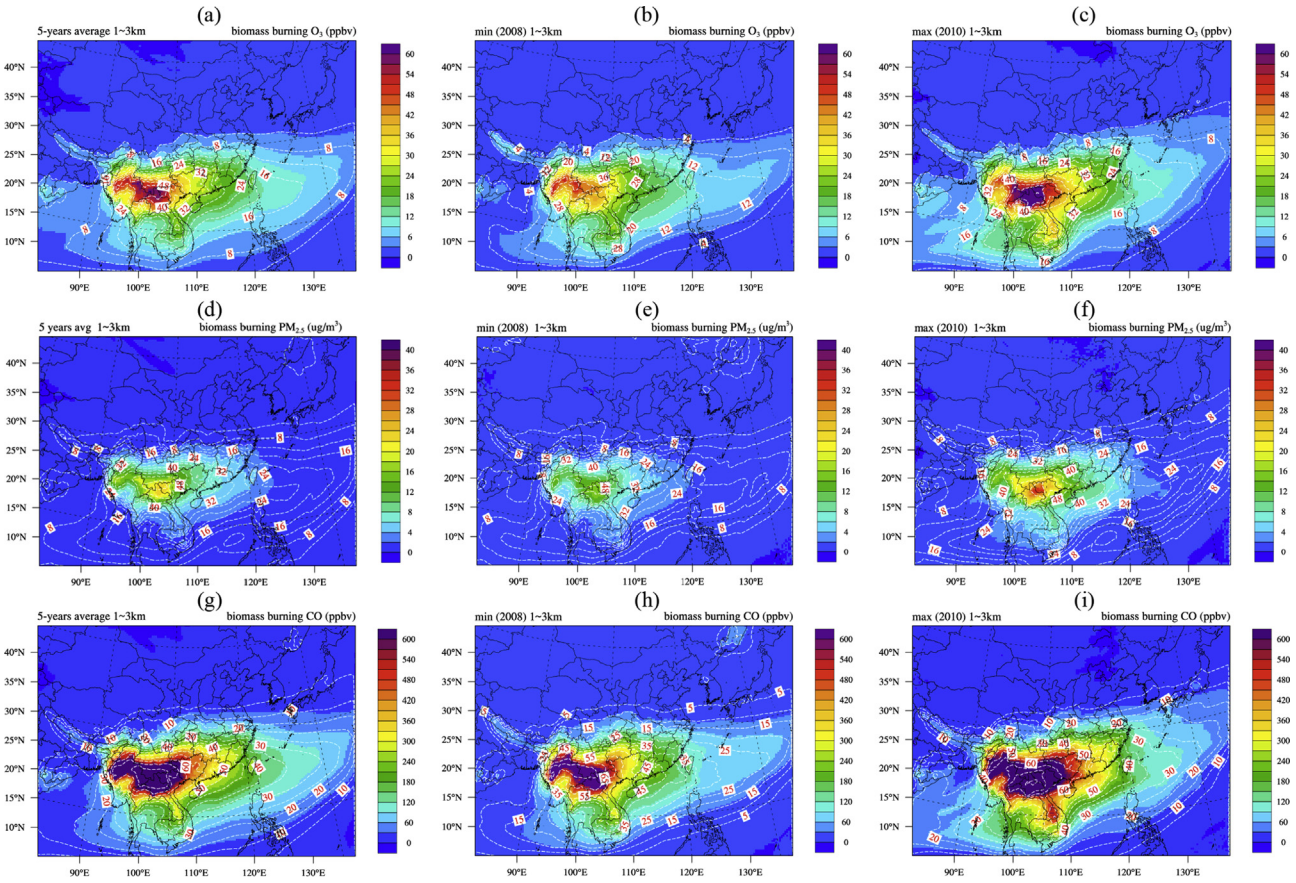

Fig. 5. Same as Fig. 3 but for lower part of free troposphere at 1 km–3 km.

atmosphere levels have large variations at downwind areas due to biomass burning emission changes at PSEA. In 2010, the contribution of O_3 was 60%–100% higher than that in 2008. Contributions for $PM_{2.5}$ and CO in higher atmosphere are similar to O_3 in terms of both spatial distribution and annual variations as illustrated in Fig. 4. At source area, contributions during different years generally agreed with the emission variations for both lower and higher atmosphere levels. But at downwind areas South China and West Pacific, only the higher atmosphere shows consistent annual variations with the perturbation of emission. While the O_3 flux analysis demonstrated excessive biomass burning plume was uplifted into free troposphere, it also suggested that most of the plume stay in higher atmosphere during the eastward transport with very limited downward flux into near surface layer. Thus the emission perturbation will mainly result in different influences in higher atmosphere over downwind areas, and the long-range transport impacts below 1 km had less variability as compared to the emission changes.

To better understand the uplift and long-range transport of biomass burning at different atmosphere levels, sounding data from Central Weather Bureau (CWB) at Taiwan was utilized to compare the O_3 profiles during strong and weak biomass burning episodes. Fig. 6 summarized the cross-sectional O_3 concentrations contributed by biomass burning (BASE-NOBIO) following the brown lineAB in Fig. 2(e). A strong biomass burning episode at Mar.7th 2007 was shown in Fig. 6(a) and a weak biomass burning episode at Mar.12th 2008 was shown in Fig. 6(b). Simulations from BASE (denoted as solid black lines) and NOBIO (denoted as dash gray lines) cases were also demonstrated in the figures. As shown in Fig. 6(c) and (d), model simulated O_3 concentrations from BASE and NOBIO cases were very close at near surface layer (0–1 km) during both episodes, suggesting the impact from PSEA biomass burning at Taiwan was limited and had little variability. At the higher atmosphere levels however, large difference between BASE and NOBIO was found. Sounding profiles also suggested significant contributions from biomass burning for the 1 km–6 km height atmosphere in Taiwan. On Mar.7th 2007, average O_3 concentrations within 0-km height from BASE and NOBIO were 31.2 ppbv and 31.3 ppbv respectively, indicating the near surface O_3 had almost no impact from PSEA biomass burning. At 1 km–6 km height however, average O_3 concentrations from BASE and NOBIO were 61.8 ppbv and 46.9 ppbv respectively, suggesting significant contribution from PSEA biomass burning by 30% for the total O_3. Elevated O_3 in higher atmosphere due to PSEA biomass burning was also found for Mar.12th 2008, but with smaller intensity as shown by Fig. 6(d). Both episodes demonstrated that major influence of PSEA biomass burning was located within lower part of free troposphere at 1 km–6 km, and massive burning events may cause greater influence in the higher atmosphere level.

Fu et al. (2012) reported the 2006 PSEA biomass burning over East Asia in surface layer could reach to 8 ppbv–18 ppbv, 160 ppbv–360 ppbv, and 8 $\mu g/m^3$–64 $\mu g/m^3$ for O_3, CO and $PM_{2.5}$ respectively; Tang et al. (2003) reported the 2001 biomass burning net influence on O_3 was about 10 ppbv for the layers below 1 km over East Asia. These studies were conducted for different years, yet the estimated contributions of biomass burning are fairly consistent with our results for the 5-years averages. As both 2001 and 2006 are estimated as having relatively moderate biomass burning emission (van der Werf et al., 2006; van der Werf et al., 2010), to our knowledge our study the first time examined the upper and lower

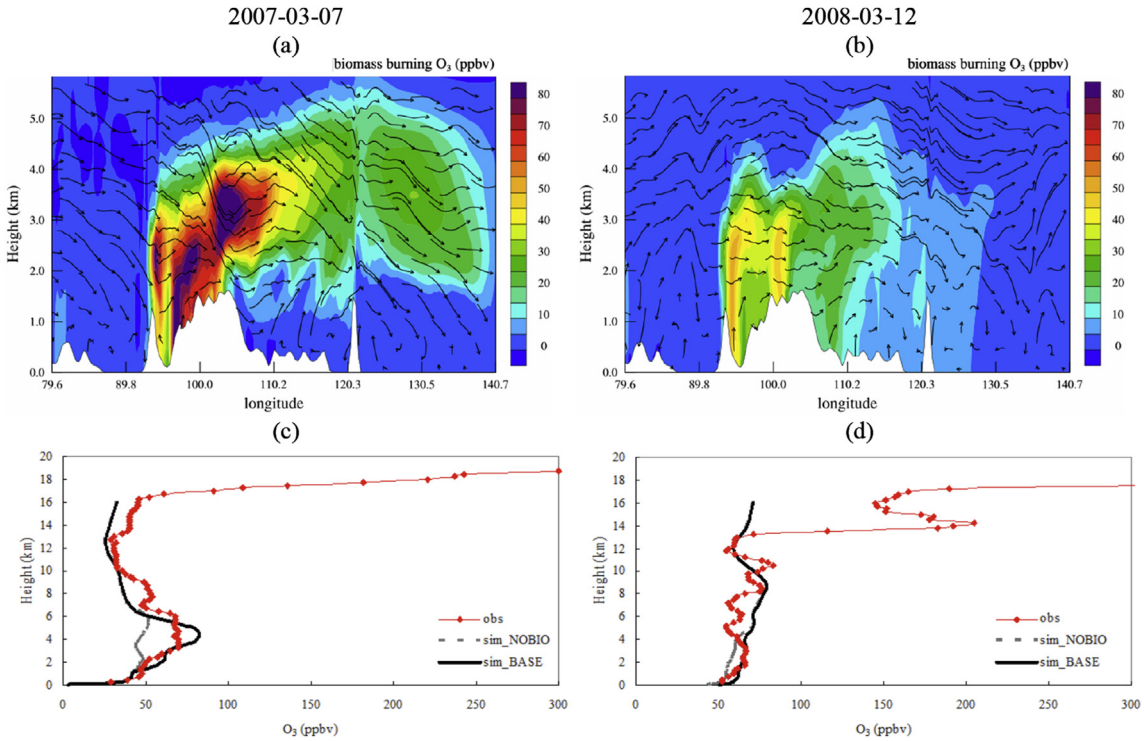

Fig. 6. Cross section of biomass burning O3 (color contours) and wind fields (black vectors) following lineAB in Fig. 2(e) for (a) Mar.7th, 2007 and (b)Mar.12th, 2008; O3 vertical profiles from CWB sounding observations (red lines with markers) and CMAQ BASE (solid black lines) and NOBIO (dash gray lines) simulations at (c) Mar.7th, 2007 and (d)Mar.12th, 2008. (For interpretation of the references to color in this figure legend, the reader is referred to the web version of this article.)

boundaries represented by 2008 and 2010, and found the significant variations of biomass burning impacts in lower part of free troposphere at downwind areas. The modeling results from our study suggested that at near surface layer below 1 km, eastward transport only carried small part of PSEA biomass burning and was partly blocked along the southeastern edge of Yungui Plateau due to impacts from Western Pacific Subtropical High. So the most significant impact was found at the conjunctions between east Myanmar, north Thailand, Yunnan Province of China, Laos and Vietnam. While in the higher atmosphere with 1 km–3 km height above surface ground, excessive gas and aerosols were uplifted and spread over South China and West Pacific without topographical boundaries, where the influences were more sensitive to emission changes from PSEA.

3.3. *Impact of biomass burning on AOD*

With enhanced gas and aerosols in higher atmosphere, the aerosol optical properties over downwind areas may also change accordingly. In this section we examined the impacts of PSEA biomass burning on AOD as shown in Fig. 7. AOD from CMAQ was prepared following the approach described in Fu et al. (2012). Spatial distributions of biomass burning AOD showed the highest impact at source region including east Myanmar, north Thailand, Laos and north Vietnam which contributed up to 70% of the total AOD. Impact of biomass burning decreased gradually along the transport pathway in downwind areas, with about 40%–60% contribution over South China and 10%–40% contribution over West Pacific on 5-years average as indicated by Fig. 7(a). While section 3.2 suggested the $PM_{2.5}$ contributions from biomass burning ranged from 8% to 24% below 1 km and 16–32% at 1 km–3 km height, impact of biomass burning had a more significant proportion contribution for AOD, which should due to the absorbing aerosol emissions from biomass burning such as black carbon and organic carbon. 2008 and 2010 were also selected to represent the upper and lower limit of impact on AOD during the 5 simulation years as shown in Fig. 7 (b) and (c) respectively. Annual changes of biomass burning AOD from different years demonstrated that AOD was sensitive to emission changes in PSEA at both source and downwind areas. Biomass burning AOD ranges from 0.2 to 0.5 (25%–55%) at source area in 2008 to 0.2–0.9 (25%–70%) in 2010, which was consistent with the emission difference between these two years. Over downwind area, lower limit of biomass burning impact in 2008 was 0.1–0.3 (25%–45%), and upper limit in 2010 was 0.3–0.8 (50%–70%).

Observations from AERONET (Holben et al., 2001) also indicated notable annual changes at different stations as summarized in Fig. 8. Daily averages of AOD from BASE case simulation (black lines: sim_BASE) and the contribution from biomass burning (blue lines: sim_BB) were also summarized to reveal the impact and its annual changes reproduced by model. Chinagmai was located at north Thailand and was the closest station to biomass burning source area, thus the AOD variations at Chiangmai represented the variability of AOD as result of the emission changes. Simulations indicated the contributions from biomass burning to the total AOD ranged from 0.21(36%) in 2008 to 0.41(71%) in 2010 which was consistent with emission changes. Despite the systematic underestimation by 40%–60% due to uncertainties from both biomass burning and anthropogenic emission inventories, both the total simulated AOD and the biomass burning AOD demonstrated large variability from year to year and AERONET observations showed similar temporal change pattern as demonstrated in Fig. 8(a). At Hong Kong (Poly Univ. station) and Taipei as shown in Fig. 8(b) and (c), contributions from biomass burning ranged from 0.27(37%) and 0.12(23%) in 2008 to 0.49(57%) and 0.23(39%) in 2010. The impact of PSEA biomass burning still played important role for enhanced AOD

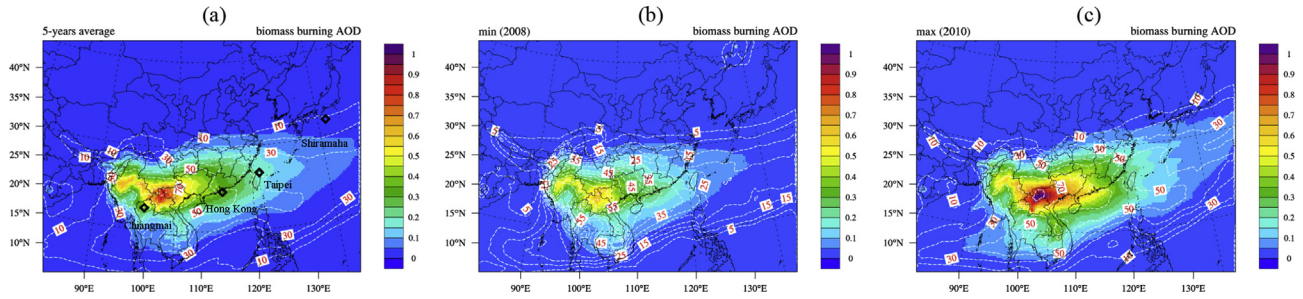

Fig. 7. Biomass burning contribution for AOD at (a) 5-years average (diamonds indicated the locations of 4 cities including Chiangmai, Hong Kong, Taipei and Shirahama.) (b) 2008 and (c) 2010. AOD values are plotted with filled color contours and percentage contributions are denoted by white dash lines with red labels. (For interpretation of the references to color in this figure legend, the reader is referred to the web version of this article.)

values at these downwind areas, but gradually declined along the transport pathway, with the annual variability also diminished with distance. At Shirahama (Japan), contribution from biomass burning for total AOD was only 0.01(2%) in 2008 and 0.04(15%) in 2010, indicating the limited impact of biomass burning at West Pacific. But some extreme values of daily AOD in 2007 and 2010 shown in Fig. 8(d) also suggested that the PSEA biomass burning can comprise more than 50% of the total AOD at Shirahama, suggesting that long-range transport also dominate the local AOD during massive burning events.

4. Conclusion

PSEA biomass burning in 5 consecutive years was investigated to assess its annual variability, transport schemes, and impact at different atmosphere levels. The analysis of emission changes revealed the significant variations of biomass burning from year to year can reach up to 65% difference in PSEA, which should partly due to the changes of precipitation. However, PSEA biomass burning impacts on the air quality at near surface layer over down wind area was found to have less variability from year to year: on 5-year average PSEA biomass burning contributions for O_3, $PM_{2.5}$, and CO were 20 ppbv–60 ppbv (10%–50%), 15 μg/m^3–35 μg/m^3 (25%–50%), 400 ppbv–600 ppbv (35%–60%) respectively at source region, 8 ppbv–26 ppbv (12%–24%), 5 μg/m^3–8 μg/m^3 (16%–20%), and 200 ppbv–300 ppbv (20%–35%) at South China, and 5 ppbv–10 ppbv (4%–12%), 0–5 μg/m^3 (0%–16%), 50 ppbv–150 ppbv (5%–30%) at West Pacific. At lower part of free troposphere within 1–3 km, interannual changes of biomass burning emission lead to large variation of pollutants concentrations over EA. The lower and upper limit impacts at EA for O_3, $PM_{2.5}$ and CO were 0–25 ppbv (0–30%), 2 μg/m^3–10 μg/m^3 (5%–25%), and 50 ppbv–300 ppbv (25%–50%) respectively in 2008, and 5 ppbv–40 ppbv (5%–45%), 5 μg/m^3–20 μg/m^3 (10%–45%), 90 ppbv–550 ppbv (30%–60%) respectively in 2010.

In this study, examination of the GPH at 850 hPa and 700 hPa demonstrated that the lee side trough along eastern flank of Tibet Plateau was the dominant contributor for uplifting PSEA biomass burning into free troposphere which further facilitate the long-range transport along South China to West Pacific, and NASA LIS/OTD data suggested that deep convection was weak over PSEA during the biomass burning season thus may only played a minor role for uplifting. This uplift motion leads to substantial loading of air pollutants into the free troposphere over downwind areas at EA. Although these pollutants had little chance of downward transport to ground surface except over Taiwan due to its high topography, it may significantly change the oxidizing capacity and optical properties in free troposphere. Due to its high terrain elevation, O_3 concentration in lower part of free troposphere at Taiwan was vulnerable to emission changes from PSEA, where the contributions can reach up to 30% in the 1 km–6 km height. But the impact on surface air quality would be very limited without strong downward drag. Analysis with AERONET observations and modeling result suggested that impact of PSEA biomass burning on AOD ranged from 0.1 to 0.3 (25%–45%) in 2008 to 0.2–0.6 (50%–70%) in 2010 over EA, which may have important effect on the underlying ground surface temperature and radiative forcing budget and need further investigations.

As one of the most important sources for both gaseous and aerosol pollutants, biomass burning in PSEA deserves the attention to fully understand its characteristics since it affects billions of population in SEA and EA. Thus understanding the contributions

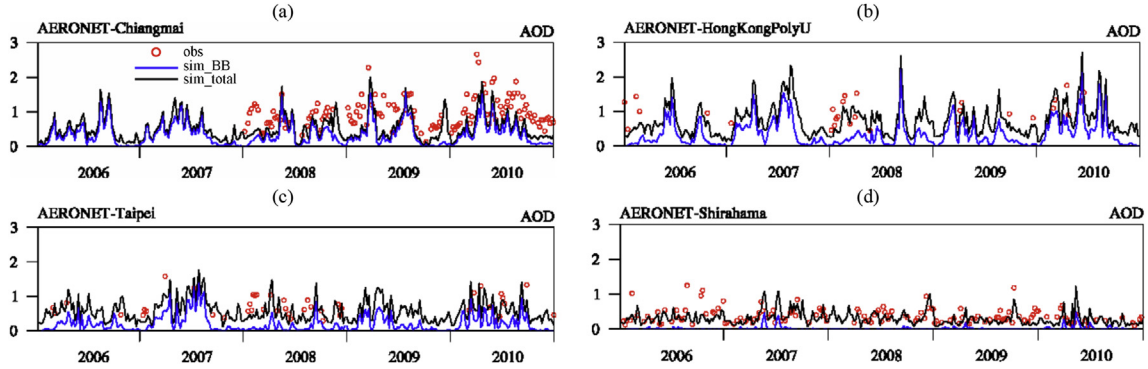

Fig. 8. Daily average AOD during March and April in 2006–2010 for BASE scenario (black lines: sim_total), contributions from biomass burning (blue lines: sim_BB) and AERONET observations (red cycles) at (a) Chiangmai (Thailand); (b) Hong Kong (South China); (c) Taipei (Taiwan); and (d) Shirahama (Japan). Locations of these 4 cities were marked in Fig. 7(a). (For interpretation of the references to color in this figure legend, the reader is referred to the web version of this article.)

from other sources such as biomass burning would greatly help these countries to better manage and evaluate their control measurements. Moreover, although this study revealed the uplifted biomass burning plumes cause substantial loadings of gas and aerosols into free troposphere, their impact on regional climate change and monsoon system remains unknown, and it is important to address these uncertainties and examine the connections between biomass burning and regional climate in future work.

Acknowledgment

We thank NASA GSFC on funding support (grant No.: NNX09AG75G). We would like to acknowledge Edward J. Hyer for providing biomass burning emission. We thank Dr. Keiichi Sato and Dr.Ayako Aoyagi from Asia Center for Air Pollution Research for providing the EANET data. We also would like to acknowledge Thailand PCD, China MEP, Taiwan EPA and CWB, Hong Kong EPD for providing the observation data, and thank NASA for providing AERONET, OMI, MODIS, and LIS/OTD data. We thank National Institude for Computational Sciences (NICS) for providing the computer sources for model simulations of this research.

References

Byun, D., Schere, K.L., 2006. Review of the governing equations, computational algorithms, and other components of the models-3 Community Multiscale Air Quality (CMAQ) modeling system. Appl. Mech. Rev. 59, 51–77.

Cook, B.I., Buckley, B.M., 2009. Objective determination of monsoon season onset, withdrawal, and length. J. Geophys. Res.-Atmos. 114.

Deng, X.J., Tie, X.X., Zhou, X.J., Wo, D., Zhong, L.J., Tan, H.B., Li, F., Huang, X.Y., Bi, X.Y., Deng, T., 2008. Effects of Southeast Asia biomass burning on aerosols and ozone concentrations over the Pearl River Delta (PRD) region. Atmos. Environ. 42, 8493–8501.

Dong, X.Y., Fu, J.S., 2015. Understanding interannual variations of biomass burning from Peninsular Southeast Asia, part I: model evaluation and analysis of systematic bias. Atmos. Environ.

Fu, J.S., Hsu, N.C., Gao, Y., Huang, K., Li, C., Lin, N.H., Tsay, S.C., 2012. Evaluating the influences of biomass burning during 2006 BASE-ASIA: a regional chemical transport modeling. Atmos. Chem. Phys. 12, 3837–3855.

Halmer, M.M., Schmincke, H.U., Graf, H.F., 2002. The annual volcanic gas input into the atmosphere, in particular into the stratosphere: a global data set for the past 100 years. J. Volcanol. Geotherm. Res. 115, 511–528.

Holben, B.N., Tanre, D., Simrnov, A., Eck, T.F., Slutsker, I., Abuhassan, N., Newcomb, W.W., Schafer, J.S., Chatenet, B., Lavenu, F., Kaufman, Y.J., Castel, J.V., Setzer, A., Markham, B., Clark, D., Frouin, R., Halthore, R., Karneli, A., O'Neill, N.T., Pietras, C., Pinker, R.T., Voss, K., Zibordi, G., 2001. An emerging ground based aerosol climatology: aerosol optical depth from AERONET. Geophys Res. Lett. 106, 12067–12097.

Huang, K., Fu, J.S., Hsu, N.C., Gao, Y., Dong, X.Y., Tsay, S.C., Lam, Y.F., 2013. Impact assessment of biomass burning on air quality in Southeast and East Asia during BASE-ASIA. Atmos. Environ. 78, 291–302.

IPCC, 2007. Contribution of Working Group I to the Fourth Assessment Report of the Intergovernmental Panel on Climate Change. New York.

Jacob, D.J., Crawford, J.H., Kleb, M.M., Connors, V.S., Bendura, R.J., Raper, J.L., Sachse, G.W., Gille, J.C., Emmons, L., Heald, C.L., 2003. Transport and Chemical Evolution over the Pacific (TRACE-P) aircraft mission: design, execution, and first results. J. Geophys. Res.-Atmos. 108, 1–19.

Jian, Y., Fu, T.M., 2014. Injection heights of springtime biomass-burning plumes over peninsular Southeast Asia and their impacts on long-range pollutant transport. Atmos. Chem. Phys. 14, 3977–3989.

Li, C., Tsay, S.C., Hsu, N.C., Kim, J.Y., Howell, S.G., Huebert, B.J., Ji, Q., Jeong, M.J., Wang, S.H., Hansell, R.A., Bell, S.W., 2013. Characteristics and composition of atmospheric aerosols in Phimai, central Thailand during BASE-ASIA. Atmos. Environ. 78, 60–71.

Lin, C.Y., Hsu, H.M., Lee, Y.H., Kuo, C.H., Sheng, Y.F., Chu, D.A., 2009. A new transport mechanism of biomass burning from Indochina as identified by modeling studies. Atmos. Chem. Phys. 9, 7901–7911.

Lin, N.H., Tsay, S.C., Maring, H.B., Yen, M.C., Sheu, G.R., Wang, S.H., Chi, K.H., Chuang, M.T., Ou-Yang, C.F., Fu, J.S., Reid, J.S., Lee, C.T., Wang, L.C., Wang, J.L., Hsu, C.N., Sayer, A.M., Holben, B.N., Chu, Y.C., Nguyen, X.A., Sopajaree, K., Chen, S.J., Cheng, M.T., Tsuang, B.J., Tsai, C.J., Peng, C.M., Schnell, R.C., Conway, T., Chang, C.T., Lin, K.S., Tsai, Y.I., Lee, W.J., Chang, S.C., Liu, J.J., Chiang, W.L., Huang, S.J., Lin, T.H., Liu, G.R., 2013. An overview of regional experiments on biomass burning aerosols and related pollutants in Southeast Asia: from BASE-ASIA and the Dongsha Experiment to 7-SEAS. Atmos. Environ. 78, 1–19.

Liu, H.Y., Jacob, D.J., Bey, I., Yantosca, R.M., Duncan, B.N., Sachse, G.W., 2003. Transport pathways for Asian pollution outflow over the Pacific: interannual and seasonal variations. J. Geophys. Res.-Atmos. 108.

Nakajima, T., Yoon, S.C., Ramanathan, V., Shi, G.Y., Takemura, T., Higurashi, A., Takamura, T., Aoki, K., Sohn, B.J., Kim, S.W., Tsuruta, H., Sugimoto, N., Shimizu, A., Tanimoto, H., Sawa, Y., Lin, N.H., Lee, C.T., Goto, D., Schutgens, N., 2007. Overview of the Atmospheric Brown Cloud East Asian Regional Experiment 2005 and a study of the aerosol direct radiative forcing in east Asia. J. Geophys. Res.-Atmos. 112.

Nho, E.Y., LeCloarec, M.F., Ardouin, B., Tjetjep, W.S., 1996. Source strength assessment of volcanic trace elements emitted from the Indonesian arc. J. Volcanol. Geotherm. Res. 74, 121–129.

Nichol, J., 1998. Smoke haze in southeast Asia: a predictable recurrence (vol. 32, pg 2715, 1998). Atmos. Environ. 32, 3917–3917.

Reid, J.S., Hyer, E.J., Johnson, R.S., Holben, B.N., Yokelson, R.J., Zhang, J.L., Campbell, J.R., Christopher, S.A., Di Girolamo, L., Giglio, L., Holz, R.E., Kearney, C., Miettinen, J., Reid, E.A., Turk, F.J., Wang, J., Xian, P., Zhao, G.Y., Balasubramanian, R., Chew, B.N., Janjai, S., Lagrosas, N., Lestari, P., Lin, N.H., Mahmud, M., Nguyen, A.X., Norris, B., Oanh, N.T.K., Oo, M., Salinas, S.V., Welton, E.J., Liew, S.C., 2013. Observing and understanding the Southeast Asian aerosol system by remote sensing: an initial review and analysis for the Seven Southeast Asian Studies (7SEAS) program. Atmos. Res. 122, 403–468.

Reid, J.S., Hyer, E.J., Prins, E.M., Westphal, D.L., Zhang, J.L., Wang, J., Christopher, S.A., Curtis, C.A., Schmidt, C.C., Eleuterio, D.P., Richardson, K.A., Hoffman, J.P., 2009. Global monitoring and forecasting of biomass-burning smoke: description of and lessons from the fire locating and modeling of burning emissions (FLAMBE) program. IEEE J. Sel. Top. Appl. Earth Obs. Remote Sens. 2, 144–162.

Reid, J.S., Xian, P., Hyer, E.J., Flatau, M.K., Ramirez, E.M., Turk, F.J., Sampson, C.R., Zhang, C., Fukada, E.M., Maloney, E.D., 2012. Multi-scale meteorological conceptual analysis of observed active fire hotspot activity and smoke optical depth in the Maritime Continent. Atmos. Chem. Phys. 12, 2117–2147.

Skamarock, W.C., Klemp, J.B., Dudhia, J., Gill, D.O., Barker, D.M., Duda, M.G., Huang, X.Y., Wang, W., Powers, J.G., 2008. A Description of the Advanced Research WRF Version 3. NCAR.

Symonds, R.B., Rose, W.I., Reed, M.H., Lichte, F.E., Finnegan, D.L., 1987. Volatilization, transport and sublimation of metallic and nonmetallic elements in high-temperature gases at Merapi-Volcano, Indonesia. Geochim. Cosmochim. Acta 51, 2083–2101.

Tang, Y.H., Carmichael, G.R., Woo, J.H., Thongboonchoo, N., Kurata, G., Uno, I., Streets, D.G., Blake, D.R., Weber, R.J., Talbot, R.W., Kondo, Y., Singh, H.B., Wang, T., 2003. Influences of biomass burning during the Transport and Chemical Evolution over the Pacific (TRACE-P) experiment identified by the regional chemical transport model. J. Geophys. Res.-Atmos. 108.

Torres, O., Chen, Z., Jethva, H., Ahn, C., Freitas, S.R., Bhartia, P.K., 2010. OMI and MODIS observations of the anomalous 2008–2009 Southern Hemisphere biomass burning seasons. Atmos. Chem. Phys. 10, 3505–3513.

Tsai, Y.I., Sopajaree, K., Chotruksa, A., Wu, H.C., Kuo, S.C., 2013. Source indicators of biomass burning associated with inorganic salts and carboxylates in dry season ambient aerosol in Chiang Mai Basin, Thailand. Atmos. Environ. 78, 93–104.

van der Werf, G.R., Dempewolf, J., Trigg, S.N., Randerson, J.T., Kasibhatla, P.S., Giglio, L., Murdiyarso, D., Peters, W., Morton, D.C., Collatz, G.J., Dolman, A.J., DeFries, R.S., 2008. Climate regulation of fire emissions and deforestation in equatorial Asia. Proc. Natl. Acad. Sci. U. S. A. 105, 20350–20355.

van der Werf, G.R., Randerson, J.T., Collatz, G.J., Giglio, L., Kasibhatla, P.S., Arellano, A.F., Olsen, S.C., Kasischke, E.S., 2004. Continental-scale partitioning of fire emissions during the 1997 to 2001 El Nino/La Nina period. Science 303, 73–76.

van der Werf, G.R., Randerson, J.T., Giglio, L., Collatz, G.J., Kasibhatla, P.S., Arellano, A.F., 2006. Interannual variability in global biomass burning emissions from 1997 to 2004. Atmos. Chem. Phys. 6, 3423–3441.

van der Werf, G.R., Randerson, J.T., Giglio, L., Collatz, G.J., Mu, M., Kasibhatla, P.S., Morton, D.C., DeFries, R.S., Jin, Y., van Leeuwen, T.T., 2010. Global fire emissions and the contribution of deforestation, savanna, forest, agricultural, and peat fires (1997–2009). Atmos. Chem. Phys. 10, 11707–11735.